ISSN 1995-0802, Lobachevskii Journal of Mathematics, 2016, Vol. 37, No. 5, pp. 570–581. © Pleiades Publishing, Ltd., 2016.

Nonlinear Finite Volume Method with Discrete Maximum Principle for the Two-Phase Flow Model

K. Nikitin[1*], K. Novikov[1,2], and Y. Vassilevski[1,2,3***]**

(Submitted by A. V. Lapin)

[1] *Institute of Numerical Mathematics, Russian Academy of Sciences, ul. Gubkina 8, Moscow, 119333 Russia*

[2] *Lomonosov Moscow State University, GSP-1, Moscow, 119991 Russia*

[3] *Moscow Institute of Physics and Technology, Institutskii per. 9, Dolgoprudny, Moscow oblast, 141700 Russia*

Received January 12, 2016

Abstract—The discrete maximum principle is a meaningful requirement for numerical schemes used in multiphase flow models. It eliminates numerical pressure overshoots and undershoots, which may cause unnatural Darcy velocities and wrong numerical saturations. In this paper we study the application of the nonlinear finite volume method with discrete maximum principle [1] to the two-phase flow model. The method satisfies the discrete maximum principle for numerical pressures of incompressible fluids with neglected capillary pressure. For non-zero capillary pressure and constant phase viscosities the discrete maximum principle holds for numerical global pressure.

DOI: 10.1134/S1995080216050097

Keywords and phrases: *Maximum principle, finite volume method, incompressible fluid.*

1. INTRODUCTION

The discrete maximum principle is a very desirable property of numerical schemes used for discretization of numerical models dealing with concentrations, densities, absolute temperatures. It provides non-negativity of solution and eliminates artificial sources and sinks. In multiphase flow models pressure gradient appears to be the main source of transport. Thus erroneous local extremum leads to wrong transport terms and consequently to wrong numerical solutions.

In this article we adapt nonlinear multi-point flux discretization scheme presented in [1, 2] for two-phase flow model. In the second section we describe the discretization scheme in application to diffusion equation. Two-phase flow model and fully implicit scheme for it are described in the third and fourth sections, respectively. Then we prove that nonlinear multi-point flux discretization for the two-phase flow model leads to solution satisfying the discrete maximum principle. Then the Jacobian of the model residuals is computed and Newton iterations are described. Finally we present numerical experiments validating the discrete maximum principle of the solution. The solution is compared with solutions obtained using two-point linear and nonlinear schemes [4].

[*] E-mail: Nikitin.Kira@gmail.com
[**] E-mail: Konst.Novikov@gmail.com
[***] E-mail: Yuri.Vassilevski@gmail.com

2. NONLINEAR MULTI-POINT FINITE VOLUME FLUX DISCRETIZATION

In this section we describe nonlinear multi-point flux discretization scheme (see [1, 2]) in application to diffusion problem.

Let Ω be a three-dimensional polyhedral domain with the Lipschitz boundary $\Gamma = \Gamma_N \cup \Gamma_D$. The diffusion equation for unknown variable p with the Dirichlet or Neumann boundary conditions written in a mixed form reads:

$$\begin{gathered} \mathbf{q} = -\mathbb{K}\nabla p, \qquad \operatorname{div} \mathbf{q} = g \quad \text{in} \quad \Omega, \\ p = g_D \quad \text{on} \quad \Gamma_D, \\ \mathbf{n} \cdot \mathbf{q} = g_N \quad \text{on} \quad \Gamma_N. \end{gathered} \tag{1}$$

Here $\mathbb{K}(\mathbf{x})$ is a symmetric positive definite (possibly anisotropic) diffusion tensor, $f(\mathbf{x})$ is a source term, $g_D(\mathbf{x})$ and $g_N(\mathbf{x})$ are given Dirichlet and Neumann boundary conditions for Γ_D and Γ_N parts of the boundary, respectively.

The weak maximum principle [6] for elliptic problems implies the maximum principle for diffusion equation solution. The last one states that for $f \leq 0$ the variable $p(\mathbf{x})$ satisfies:

$$\max_{\mathbf{x}\in\bar{\Omega}} p(\mathbf{x}) \leq \max_{\mathbf{x}\in\Gamma_D\cup\Gamma_N} p(\mathbf{x}).$$

The minimum principle is formulated accordingly: for $f \geq 0$ the pressure $p(\mathbf{x})$ satisfies:

$$\min_{\mathbf{x}\in\bar{\Omega}} p(\mathbf{x}) \geq \min_{\mathbf{x}\in\Gamma_D\cup\Gamma_N} p(\mathbf{x}).$$

Note, that if $g_N \geq 0$ then the maximum principle states additionally, that p cannot attain maximum on Γ_N. If $g_N \leq 0$ then p cannot attain minimum on Γ_N.

2.1. Nonlinear FV Discretization Scheme

The FV scheme uses one degree of freedom per cell T, p_T, collocated at cell barycenter $\mathbf{x}_T$. Integrating the mass balance equation (1) over T and using the divergence theorem, we obtain:

$$\sum_{f\in\partial T} \sigma_{T,f}\mathbf{q}_f \cdot \mathbf{n}_f = \int_T g \mathrm{d}x, \qquad \mathbf{q}_f = \frac{1}{|f|}\int_f \mathbf{q}\mathrm{d}s,$$

where $\mathbf{q}_f \cdot \mathbf{n}_f$ is the total flux across face f, and $\sigma_{T,f}$ is either 1 or -1 depending on the mutual orientation of the normal vectors $\mathbf{n}_f$ and $\mathbf{n}_T$ ($\mathbf{n}_T$ denotes the outward normal vector), $|n_f| = |f|$ and $|f|$ denotes area of face f.

Both nonlinear discretization schemes (multi-point and two-point) exploit the same idea. The monotone two-point scheme was described in details in [3, 4]. Here we describe only the multi-point discretization.

2.2. Multi-Point Flux Discretization

First for each cell-face pair we need to find a triplet (see Fig. 1 for a 2D example), a set of three vectors $\mathbf{t}_*$ such that for the co-normal vector $l_f = \mathbb{K} \cdot \mathbf{n}_f$ we have

$$l_f = \alpha\, \mathbf{t}_1 + \beta\, \mathbf{t}_2 + \gamma\, \mathbf{t}_3, \tag{2}$$

where coefficients α, β and γ are non-negative.

Since the flux normal component is in fact the directional derivative along the co-normal vector l_f, it can also be represented as the sum of three derivatives along $\mathbf{t}_*$ which are approximated by central differences:

$$q_+ = \alpha'_+(p_+ - p_{+,1}) + \beta'_+(p_+ - p_{+,2}) + \gamma'_+(p_+ - p_{+,3}), \tag{3}$$

where coefficients α'_+, β'_+, γ'_+ are normalized by $|t_{+,i}|/|l_f|$ coefficients (2) for cell T_+.

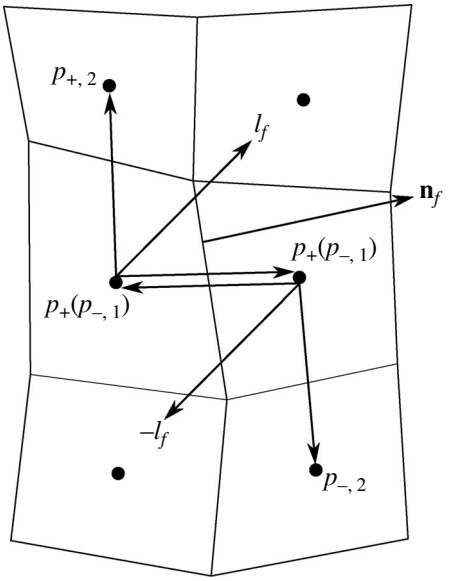

Fig. 1. Two representations of co-normal vector $l_f = \mathbb{K} \cdot \mathbf{n}_f$ (2D example).

For the opposite co-normal vector $-l_f$ we have the similar representation with non-negative coefficients:

$$q_- = \alpha'_-(p_- - p_{-,1}) + \beta'_-(p_- - p_{-,2}) + \gamma'_-(p_- - p_{-,3}). \tag{4}$$

Now we can take a linear combination of (3) and (4) with non-negative coefficients μ_+ and μ_-:

$$\mathbf{q}_f \cdot \mathbf{n}_f = \mu_+ q_+ + \mu_-(-q_-). \tag{5}$$

Flux approximation requires the linear combination of μ_+, μ_- to be convex:

$$\mu_+ + \mu_- = 1. \tag{6}$$

To construct the *multi-point* nonlinear discretization, we set equal two representations of the flux:

$$\mu_+ q_+ = -\mu_- q_-. \tag{7}$$

The solution of equations (6) and (7) for 2D case is considered in detail in [1]. Here we use these results in 3D case.

If $|q_+| = |q_-| = 0$ then the solution of (6), (7) is not unique. In this case we choose $\mu_+ = \mu_- = 1/2$. Otherwise consider two cases. The first case is for $q_+ q_- \le 0$. The solution is

$$\mu_+ = \frac{q_-}{q_- - q_+}, \qquad \mu_- = \frac{q_+}{q_+ - q_-},$$

and $\mu_\pm$ are non-negative. Thus,

$$\mathbf{q}_f \cdot \mathbf{n}_f = \frac{2q_+q_-}{q_- - q_+} = -\frac{2q_-q_+}{q_+ - q_-},$$

and numerical flux has two equivalent algebraic representations:

$$\begin{aligned}\mathbf{q}_f \cdot \mathbf{n}_f &= 2\mu_+\Big(\alpha'_+(p_+ - p_{+,1}) + \beta'_+(p_+ - p_{+,2}) + \gamma'_+(p_+ - p_{+,3})\Big)\\ &= A_{+,1}(p_+ - p_{+,1}) + A_{+,2}(p_+ - p_{+,2}) + A_{+,3}(p_+ - p_{+,3}),\end{aligned}$$

and

$$\begin{aligned}-\mathbf{q}_f \cdot \mathbf{n}_f &= 2\mu_-\Big(\alpha'_-(p_- - p_{-,1}) + \beta'_-(p_- - p_{-,2}) + \gamma'_-(p_- - p_{-,3})\Big)\\ &= A_{-,1}(p_- - p_{-,1}) + A_{-,2}(p_- - p_{-,2}) + A_{-,3}(p_- - p_{-,3}),\end{aligned}$$

with non-negative coefficients $A_{\pm,k}$, $k = 1, 2, 3$. Note that these coefficients depend on fluxes and hence on values of p at neighboring cells. Thus, the resulting multi-point flux approximation is *nonlinear* and its stencil is embedded into the set of the closest neighboring cells.

The second case, $q_+q_- > 0$, leads to a potentially degenerate diffusive flux. In order to avoid this degeneracy, the authors in [5] re-group the terms in equation (5) as follows:

$$\mathbf{q}_f \cdot \mathbf{n}_f = \mu_+\widetilde{q}_+ + \mu_-(-\widetilde{q}_-) + (\mu_+\alpha'_+ + \mu_-\alpha'_-)(p_+ - p_-),$$

where $\widetilde{q}_+ = \beta'_+(p_+ - p_{+,2}) + \gamma'_+(p_+ - p_{+,3})$, $\widetilde{q}_- = \beta'_-(p_- - p_{-,2}) + \gamma'_-(p_- - p_{-,3})$.

We find μ_+ and μ_- as a solution of

$$\widetilde{q}_+\mu_+ + \widetilde{q}_-\mu_- = 0, \qquad \mu_+ + \mu_- = 1.$$

Again if the solution is not unique, we choose $\mu_+ = \mu_- = 1/2$. Otherwise, for $\widetilde{q}_+\widetilde{q}_- \le 0$ we get

$$\begin{aligned}\mathbf{q}_f \cdot \mathbf{n}_f = 2\mu_+\widetilde{q}_+ + (\mu_+\alpha'_+ + \mu_-\alpha'_-)(p_+ - p_-) = A_{+,1}(p_+ - p_{+,1}) + A_{+,2}(p_+ - p_{+,2})\\ + A_{+,3}(p_+ - p_{+,3}) = -2\mu_-\widetilde{q}_- - (\mu_+\alpha'_+ + \mu_-\alpha'_-)(p_- - p_+)\\ = -A_{-,1}(p_- - p_{-,1}) - A_{-,2}(p_- - p_{-,2}) - A_{-,3}(p_- - p_{-,3}),\end{aligned}$$

where $A_{+,1} = A_{-,1} = \mu_+\alpha_{+,1} + \mu_-\alpha_{-,1}$. If $\widetilde{q}_+\widetilde{q}_- > 0$

$$q_f = (\mu_+\alpha'_+ + \mu_-\alpha'_-)(p_+ - p_-) = A_{+,1}(p_+ - p_-).$$

Calculating $A_{\pm,k}$ and inserting the diffusive fluxes $\mathbf{q}_f \cdot \mathbf{n}_f$ in the mass balance equation, we get an algebraic problem. For a logically cubic mesh, the considered finite volume scheme results in the conventional seven-point stencil.

3. TWO-PHASE BLACK OIL MODEL

We consider a two-phase flow of immiscible fluids in a porous medium [7, 8]. The phase, that wets the medium more than the other, is called wetting phase and is indicated by subscript w. The other phase is the non-wetting phase and indicated by o.

The basic equations for the two-phase flow are the following:

- Mass conservation for each phase:

$$\frac{\partial \phi \rho_\alpha S_\alpha}{\partial t} = -\nabla \cdot (\rho_\alpha \mathbf{u}_\alpha) + q_\alpha, \quad \alpha = w, o; \tag{8}$$

- Darcy's law:

$$\mathbf{u}_\alpha = -\frac{k_{r\alpha}}{\mu_\alpha}\mathbb{K}\left(\nabla p_\alpha - \rho_\alpha g \nabla z\right), \quad \alpha = w, o; \tag{9}$$

- Two fluids fill the voids:

$$S_w + S_o = 1; \tag{10}$$

- Pressure difference between phases is given by capillary pressure:

$$p_o - p_w = p_c(S_w), \tag{11}$$

where $\mathbb{K}$ is the absolute permeability tensor, ρ_α is the phase density, μ_α is the viscosity, $k_{r\alpha}$ is the relative phase permeability, ϕ is the porosity, g is the gravity term and q_α is the source/sink well term.

On the reservoir boundary we consider no-flow (homogeneous Neumann) condition.

Wells are introduced through one of the following conditions: either given bottom hole pressure p_{bh}, or given component flux q_α, or given total flux $q_T = q_w + q_o$ for producing wells.

All the test cases in this article were performed for vertical perfect wells. The formula for the well term was suggested by Peaceman [9]. For a cell T with center $\mathbf{x}_T$ connected to the well we have:

$$q_\alpha = \frac{k_{r\alpha}}{\mu_\alpha} WI\Big(p_{bh} - p_\alpha - \rho_\alpha g(z_{bh} - z)\Big)\delta(\mathbf{x} - \mathbf{x}_T),$$

WI is the *well index* which does not depend on the properties of fluids but depends on properties of the media, $\delta(\mathbf{x}-\mathbf{x}_T)$ is the Dirac function.

Choosing oil pressure $P=p_o$ and water saturation $S=S_w$ as primary unknowns, defining a formation volume factor $B_\alpha=\rho_{\alpha,0}/\rho_\alpha$, and mobility $\lambda_\alpha=k_{r\alpha}/(\mu_\alpha B_\alpha)$ and using (8)–(11) we can get the equivalent formulation:

$$\frac{\partial}{\partial t}\frac{\phi S}{B_w}+\nabla\cdot\mathbb{K}\lambda_w(\nabla P-\nabla P_c(S)-\frac{\rho_{w,0}}{B_w}g\nabla z)=\frac{q_w}{\rho_{w,0}},$$
$$\frac{\partial}{\partial t}\frac{\phi(1-S)}{B_o}+\nabla\cdot\mathbb{K}\lambda_o(\nabla P-\frac{\rho_{o,0}}{B_o}g\nabla z)=\frac{q_o}{\rho_{o,0}}. \tag{12}$$

In the discrete counterparts of (8),(9) the mobilities $\lambda_\alpha(S,p)$ on the face f_{ij} are taken upwinded:

$$\lambda_\alpha(S)=\begin{cases}\lambda_\alpha(S_i,p_i) & \text{if flow is directed from cell } i \text{ to cell } j,\\ \lambda_\alpha(S_j,p_j) & \text{if flow is directed from cell } j \text{ to cell } i.\end{cases}$$

The phase mobilities for well-producer are taken upwinded from the cell. For well-injector we have only water injected and thus take the downstream mobility from the cell with the well: $\lambda_{inj}=(\frac{k_{rw}}{\mu_w B_w}+\frac{k_{ro}}{\mu_o B_o})_{cell}$. We also assume that there is no capillary pressure in wells, so all the well fluxes depend on the same (oil) pressure.

4. FULLY IMPLICIT SCHEME FOR TWO-PHASE FLOW EQUATIONS

First we apply the implicit scheme to the mass conservation equations (8):

$$\frac{(\frac{\phi S_\alpha}{B_\alpha})^{n+1}-(\frac{\phi S_\alpha}{B_\alpha})^n}{\Delta t^{n+1}}=-\mathrm{div}(\mathbf{u}_\alpha^{n+1})+\left(\frac{q_\alpha}{\rho_{\alpha,0}}\right)^{n+1},\quad \alpha=w,o. \tag{13}$$

Now we can write down the nonlinear residual equations for the l^{th} approximation to a quantity evaluated at time step $n+1$ inside grid cell T_i:

$$R^l_{\alpha,i}=\int\limits_{T_i}\left[\left(\frac{\phi S_\alpha}{B_\alpha}\right)^l_i-\left(\frac{\phi S_\alpha}{B_\alpha}\right)^n_i+\Delta t^{n+1}\left(\mathrm{div}\mathbf{u}_\alpha-\frac{q_\alpha}{\rho_{\alpha,0}}\right)^l_i\right]\mathrm{d}x,\quad \alpha=w,o.$$

The discrete counterpart of (13) can be written as:

$$R_{\alpha,i}=0,\quad \alpha=w,o \tag{14}$$

for all grid cells at every time step.

5. DISCRETE MAXIMUM PRINCIPLE

In order to derive discrete maximum principle we introduce assumptions on two-phase flow model coefficients:

(a1) constant water and oil densities: $B_\alpha=1$, $\alpha=w,o$;

(a2) constant porosity: $\phi=\mathrm{const}$;

(a3) capillary pressure is neglected: $p_c\equiv 0$;

(a4) gravitational term is neglected: $u_\alpha=-\frac{k_{r\alpha}}{\mu_\alpha}\mathbb{K}(\nabla p_\alpha)$, $\alpha=w,o$.

Using summation over α in (14) and assumptions (a1)–(a4) we get

$$-\int\limits_{T_i}\mathrm{div}\,(\mathbb{K}\lambda\nabla p_o)^l dx=\int\limits_{T_i}\left(\frac{q_w}{\rho_w}+\frac{q_o}{\rho_o}\right)^l dx, \tag{15}$$

where $\lambda = \frac{k_{rw}}{B_w\mu_w} + \frac{k_{ro}}{B_o\mu_o}$. Using divergence theorem we rewrite (15):

$$\sum_{f\in\partial T} \lambda_f^l \mathbf{q}_f^l \cdot \mathbf{n}_f = \int\limits_{T_i} \left(\frac{q_w}{\rho_w} + \frac{q_o}{\rho_o}\right)^l dx,$$

where $\mathbf{n}_f$ is the exterior normal vector to face f, $|\mathbf{n}_f| = |f|$, $|f|$ is the area of face f, and $\mathbf{q}_f$ is the flux over face f. The discrete flux normal component $\mathbf{q}_f \cdot \mathbf{n}_f$ may be defined via the pressure differences according to Section 2.2:

$$\sum_{f\in\partial T} \sum_{i=1}^{3} \lambda_f^l A_{i,f}(p_T^l - p_{T,i}^l) = \int\limits_{T_i} \left(\frac{q_w}{\rho_w} + \frac{q_o}{\rho_o}\right)^l dx. \tag{16}$$

Let $\mathcal{T}$ stand for the set of all cells and $\mathcal{T}_D$ and $\mathcal{T}_N$ stand for the set of cells with Dirichlet boundary faces and Neumann boundary faces, respectively. We also denote all boundary cells by $\mathcal{T}_B = \mathcal{T}_D \cup \mathcal{T}_N$.

Theorem 1 (Discrete maximum principle) *Let the solution p to* (16) *exist. Let $\mathcal{T}_{inj}$ be the set of cells where $\frac{q_w}{\rho_w} + \frac{q_o}{\rho_o} > 0$. Then*

$$\max_{T\in\mathcal{T}\setminus(\mathcal{T}_{inj}\cup\mathcal{T}_B)} p_T \le p_{\max} = \max_{\mathcal{T}_{inj}\cup\mathcal{T}_B} p_T.$$

Proof. Assume that p_T in a cell $T \in \mathcal{T} \setminus (\mathcal{T}_{inj} \cup \mathcal{T}_B)$ has the maximum value.

Coefficients $A_{i,f}$ in (16) are nonnegative by construction. As p_T has the maximum value, from non-negativity of coefficients $A_{i,f}$ and the form of equation (16) one derives that $\mathbf{q}_f^l \cdot \mathbf{n}_f$ are non-negative. λ is a positive coefficient. Thus the left hand side of equation (16) is non-negative, and the right hand of (16) is non-positive in $\mathcal{T} \setminus (\mathcal{T}_{inj} \cup \mathcal{T}_B)$. Then both sides of the equation are equal to zero.

Since $\lambda_f \mathbf{q}_f^l \cdot \mathbf{n}_f$ are non-negative and their sum is zero, we get $\mathbf{q}_f^l \cdot \mathbf{n}_f = 0\ \forall f \in \partial T$. Since the discrete normal flux on face f contains the term $p_T - p_{T'}$ where T' is the cell neighbouring T through f, we conclude that $p_T = p_{T'}$.

Assuming that the mesh $\mathcal{T}/\mathcal{T}_{inj}$ is face-connected, we get that p is constant in $\mathcal{T} \setminus (\mathcal{T}_{inj} \cup \mathcal{T}_B)$. □

Remark 1. *If we have no-flow Neumann condition for p on face f or positive Neumann condition (outflux), flow over this face $\mathbf{q}_f^l \cdot \mathbf{n}_f$ is non-negative and the proof of the Theorem* 1 *remains correct for this case. Thus p also cannot attain maximum on Neumann boundary (otherwise $p \equiv$* const *in the whole domain).*

Remark 2. *The authors of* [1] *also construct nonlinear multi-point flux discretization for discontinious diffusion tensor $\mathbb{K}$. Under assumptions* (a1–a4) *the discrete maximum principle for solution of the two-phase flow model also holds for discontinious case. The proof is similar to the proof of the Theorem* 1.

6. NONLINEAR COEFFICIENTS VARIATION

If we use a Jacobian-based nonlinear solver, we need a variation of coefficients $A_{\pm,i}$ in flux discretizations.

First we write variations for $q_\pm$ and $\widetilde{q}_\pm$:

$$\Delta q_\pm = (\alpha'_\pm + \beta'_\pm + \gamma'_\pm)\Delta p_\pm - \alpha'_\pm \Delta p_{\pm,1} - \beta'_\pm \Delta p_{\pm,2} - \gamma'_\pm \Delta p_{\pm,3},$$

$$\Delta \widetilde{q}_\pm = (\beta'_\pm + \gamma'_\pm)\Delta p_\pm - \beta'_\pm \Delta p_{\pm,2} - \gamma'_\pm \Delta p_{\pm,3}.$$

Variations for $\mu_\pm$ and $A_{\pm,i}$ depend on the q_+, q_-. If $|q_+| + |q_-| > 0$ and $q_+ q_- \le 0$, then

$$\Delta\mu_\pm = \frac{\Delta q_\mp}{q_\mp - q_\pm} - (\Delta q_\mp - \Delta q_\pm)\frac{q_\mp}{(q_\mp - q_\pm)^2},$$

$$\Delta A_{\pm,1} = 2\alpha'_\pm \Delta\mu_\pm, \qquad \Delta A_{\pm,2} = 2\beta'_\pm \Delta\mu_\pm, \qquad \Delta A_{\pm,3} = 2\gamma'_\pm \Delta\mu_\pm.$$

Otherwise variation for $\mu_\pm$ depends on the $\widetilde{q}_+, \widetilde{q}_-$. If $|\widetilde{q}_+| + |\widetilde{q}_-| > 0$ and $\widetilde{q}_+\widetilde{q}_- \le 0$, then

$$\Delta\mu_\pm = \frac{\Delta\widetilde{q}_\mp}{\widetilde{q}_\mp - \widetilde{q}_\pm} - (\Delta\widetilde{q}_\mp - \Delta\widetilde{q}_\pm)\frac{\widetilde{q}_\mp}{(\widetilde{q}_\mp - \widetilde{q}_\pm)^2},$$

$$\Delta A_{\pm,1} = \alpha'_+\Delta\mu_+ + \alpha'_-\Delta\mu_-, \qquad \Delta A_{\pm,2} = 2\beta'_\pm\Delta\mu_\pm, \qquad \Delta A_{\pm,3} = 2\gamma'_\pm\Delta\mu_\pm.$$

If $|\widetilde{q}_+| + |\widetilde{q}_-| > 0$ and $\widetilde{q}_+\widetilde{q}_- > 0$, then

$$\Delta\mu_\pm = \frac{\Delta\widetilde{q}_\mp}{\widetilde{q}_\mp - \widetilde{q}_\pm} - (\Delta\widetilde{q}_\mp - \Delta\widetilde{q}_\pm)\frac{\widetilde{q}_\mp}{(\widetilde{q}_\mp - \widetilde{q}_\pm)^2},$$

$$\Delta A_{\pm,1} = \alpha'_+\Delta\mu_+ + \alpha'_-\Delta\mu_-, \qquad \Delta A_{\pm,2} = 0, \qquad \Delta A_{\pm,3} = 0.$$

In the case of $|q_+| = |q_-| = 0$ or $|\widetilde{q}_+| = |\widetilde{q}_-| = 0$ we refer to remark 3. The final variation for $q_\pm$ is

$$\Delta q_\pm = (A_{\pm,1} + A_{\pm,2} + A_{\pm,3})\Delta p_\pm - A_{\pm,1}\Delta p_{\pm,1} - A_{\pm,2}\Delta p_{\pm,2} - A_{\pm,3}\Delta p_{\pm,3}$$
$$+ \Delta A_{\pm,1}(p_\pm - p_{\pm,1}) + \Delta A_{\pm,2}(p_\pm - p_{\pm,2}) + \Delta A_{\pm,3}(p_\pm - p_{\pm,3}).$$

Remark 3. *Coefficients $\mu_\pm$ in case of zero fluxes $|q_+| = |q_-| = 0$ or zero modified fluxes $|\widetilde{q}_+| = |\widetilde{q}_-| = 0$ have discontinuities with respect to $p_{\pm,i}$. These cases pose a technical problem for the Newton solver. Possible solution of this problem is to induce small perturbation in the pressure field. Alternatively one can use a solver without usage of Jacobian for one timestep.*

7. NEWTON METHOD FOR TWO-PHASE FLOW MODEL

We suggest to use Newton's method to solve nonlinear system (14) with Darcy velocities (9):

$$J(x^l)\delta x^l = -R(x^l), \qquad x^{l+1} = x^l + \delta x^l,$$

where l is the l^{th} Newton step, x is a vector of primary unknowns in all grid cells,

$$x = \begin{pmatrix} p_o \\ S_w \end{pmatrix},$$

R is the vector of nonlinear residuals in all grid cells,

$$R(x) = \begin{pmatrix} R_w(x) \\ R_o(x) \end{pmatrix},$$

and J is the Jacobian matrix:

$$J(x) = \begin{pmatrix} \frac{\partial R_w}{\partial p_o}(x) & \frac{\partial R_w}{\partial S_w}(x) \\ \frac{\partial R_o}{\partial p_o}(x) & \frac{\partial R_o}{\partial S_w}(x) \end{pmatrix}.$$

We terminate Newton's method when the norm of the residual vector drops below ε_{nwt}.

Below we consider the construction of Jacobian matrix. We divide the residuals into two parts: accumulation (including well terms) and transport, $R_{\alpha,i} = R^{acc}_{\alpha,i} + R^{trans}_{\alpha,i}$, where:

$$R^{acc}_{\alpha,i} = V_i\left[\left(\frac{\phi S_\alpha}{B_\alpha}\right)^l_i - \left(\frac{\phi S_\alpha}{B_\alpha}\right)^n_i\right] - \Delta t^{n+1}\left(\frac{q_\alpha}{\rho_{\alpha,0}}\right)^l_i, \quad \alpha = w, o,$$

$$R^{trans}_{\alpha,i} = \Delta t^{n+1}\int\limits_{T_i}(\mathrm{div}\mathbf{u}_\alpha)\mathrm{d}x, \quad \alpha = w, o.$$

We also take advantage of the following dependencies:

- $S_o = 1 - S_w$ (see eq. (10));

- $p_w = p_o - p_c(S_w)$, with piecewise linear function $p_c(S_w)$ given by table data (see eq. (11));
- $k_{r\alpha} = k_{r\alpha}(S_w)$ are piecewise linear functions given by table data;
- $\mu_\alpha = \mu_\alpha(p_o)$ are piecewise linear functions given by table data;
- $B_\alpha = B_\alpha(p_o)$ are piecewise linear functions given by table data;
- $\phi = \phi(1 + c_R(p_o - p_o^0))$.

7.0.1. Accumulation term. The variation of the accumulation term is as follows:

$$\Delta R_{w,i}^{acc} = V_i \left[\Delta\left(\frac{\phi S_w}{B_w}\right)\right] - \Delta t^{n+1}\Delta\left(\frac{q_w}{\rho_{w,0}}\right),$$
$$\Delta R_{o,i}^{acc} = V_i \left[\Delta\left(\frac{\phi S_o}{B_o}\right)\right] - \Delta t^{n+1}\Delta\left(\frac{q_o}{\rho_{o,0}}\right),$$

where

$$\Delta\left(\frac{\phi S_w}{B_w}\right) = \frac{\phi}{B_w}\Delta S_w + S_w\left(\frac{c_R}{B_w} - \frac{\phi}{B_w^2}\frac{dB_w}{dp_o}\right)\Delta p_o,$$
$$\Delta\left(\frac{\phi S_o}{B_o}\right) = -\frac{\phi}{B_o}\Delta S_w + (1 - S_w)\left(\frac{c_R}{B_o} - \frac{\phi}{B_o^2}\frac{dB_o}{dp_o}\right)\Delta p_o.$$

7.0.2. Transport term. Now we consider the transport term composed of Darcy fluxes

$$R_{\alpha,i}^{trans} = \Delta t^{n+1}\int\limits_{\Gamma_i}(\mathbf{u}_\alpha\cdot\mathbf{n})\mathrm{d}s \approx \Delta t^{n+1}\sum_{f\in\Gamma_i}\mathbf{u}_{\alpha,f}\cdot\mathbf{n}_f.$$

If we use the multi-point discretization of the flux, then we have two different representations of flux over face f for two neighbouring cells $T_\pm$:

$$\begin{aligned}(\mathbf{u}_{w,f}^h\cdot\mathbf{n}_f)_\pm = &-\left(\frac{k_{rw}}{\mu_w B_w}\right)_f(A_{\pm,1}^{p_o}(p_{o,\pm}-p_{o,\pm,1}) + A_{\pm,2}^{p_o}(p_{o,\pm}-p_{o,\pm,2}) + A_{\pm,3}^{p_o}(p_{o,\pm}-p_{o,\pm,3}))\\ &+\left(\frac{k_{rw}}{\mu_w B_w}\right)_f(A_{\pm,1}^{p_c}(p_{c,\pm}-p_{c,\pm,1}) + A_{\pm,2}^{p_c}(p_{c,\pm}-p_{c,\pm,2}) + A_{\pm,3}^{p_c}(p_{c,\pm}-p_{c,\pm,3}))\\ &+\left(\frac{k_{rw}}{\mu_w B_w^2}\right)_f(\rho_{w,0}g(A_{\pm,1}^{z}(z_\pm - z_{\pm,1}) + A_{\pm,2}^{z}(z_\pm - z_{\pm,2}) + A_{\pm,3}^{z}(z_\pm - z_{\pm,3}))),\end{aligned} \tag{17}$$

$$\begin{aligned}(\mathbf{u}_{o,f}^h\cdot\mathbf{n}_f)_\pm = &-\left(\frac{k_{ro}}{\mu_o B_o}\right)_f(A_{\pm,1}^{p_o}(p_{o,\pm}-p_{o,\pm,1}) + A_{\pm,2}^{p_o}(p_{o,\pm}-p_{o,\pm,2}) + A_{\pm,3}^{p_o}(p_{o,\pm}-p_{o,\pm,3}))\\ &+\left(\frac{k_{ro}}{\mu_o B_o^2}\right)_f(\rho_{o,0}g(A_{\pm,1}^{z}(z_\pm - z_{\pm,1}) + A_{\pm,2}^{z}(z_\pm - z_{\pm,2}) + A_{\pm,3}^{z}(z_\pm - z_{\pm,3}))).\end{aligned} \tag{18}$$

Here $k_{r\alpha} = k_{r\alpha}(\widetilde{S})$, $\widetilde{S}$ is the upwinded value of water saturation on face f and $B_\alpha = B_\alpha(\widetilde{p})$, $\mu_\alpha = \mu_\alpha(\widetilde{p})$, $\widetilde{p}$ is the upwinded value of oil pressure on face f and coefficients $A_{\pm,i}$ depend on variable value in the neighbouring cells:

$$A_{\pm,i}^{p_\alpha} = A_{\pm,i}^{p_\alpha}(p_{\alpha,+,1}, p_{\alpha,+,2}, p_{\alpha,+,3}, p_{\alpha,-,1}, p_{\alpha,-,2}, p_{\alpha,-,3}),$$
$$A_{\pm,i}^{z} = A_{\pm,i}^{z}(z_{+,1}, z_{+,2}, z_{+,3}, z_{z-,1}, z_{z-,2}, z_{-,3}).$$

We define auxiliary variables and derivatives:

$$\lambda_{g,\alpha} = \frac{k_{r\alpha}}{\mu_w B_w^2}, \qquad \frac{d\lambda_{g,\alpha}}{d\widetilde{S}} = \frac{d\lambda_\alpha}{d\widetilde{S}}/B_w, \qquad \frac{d\lambda_{g,\alpha}}{d\widetilde{p}} = \left(\frac{d\lambda_\alpha}{d\widetilde{p}}B_w - \lambda_\alpha\frac{dB_w}{d\widetilde{p}}\right)/B_w^2,$$

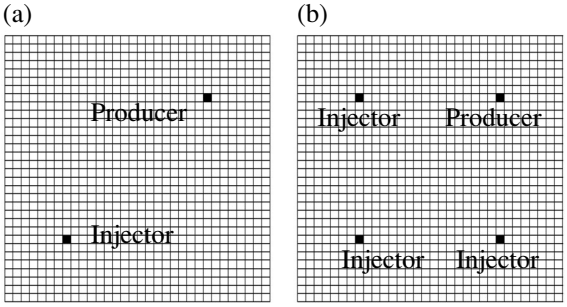

Fig. 2. Schemes of the numerical experiments.

$$\mathcal{D}_1 = A^{p_o}_{\pm,1}(p_{o,\pm} - p_{o,\pm,1}) + A^{p_o}_{\pm,2}(p_{o,\pm} - p_{o,\pm,2}) + A^{p_o}_{\pm,3}(p_{o,\pm} - p_{o,\pm,3}),$$
$$\mathcal{D}_2 = A^{p_c}_{\pm,1}(p_{c,\pm} - p_{c,\pm,1}) + A^{p_c}_{\pm,2}(p_{c,\pm} - p_{c,\pm,2}) + A^{p_c}_{\pm,3}(p_{c,\pm} - p_{c,\pm,3}),$$
$$\mathcal{D}_{3,\alpha} = \rho_{\alpha,0} g(A^{z}_{\pm,1}(z_{\pm} - z_{\pm,1}) + A^{z}_{\pm,2}(z_{\pm} - z_{\pm,2}) + A^{z}_{\pm,3}(z_{\pm} - z_{\pm,3})).$$

Using (17) and (18) we get the following representation for the flux variation for each of two phases:

$$\begin{aligned}\Delta(\mathbf{u}^h_{w,f}\cdot\mathbf{n}_f) = &\left[\left(\frac{d\lambda_w}{d\widetilde{S}_w}\right)(-\mathcal{D}_1+\mathcal{D}_2) + \frac{d\lambda_{g,w}}{d\widetilde{S}_w}\mathcal{D}_{3,w}\right]\Delta\widetilde{S}_w\\ &+\left[\left(\frac{d\lambda_w}{d\widetilde{p}_o}\right)(-\mathcal{D}_1+\mathcal{D}_2) + \frac{d\lambda_{g,w}}{d\widetilde{p}_o}\mathcal{D}_{3,w}\right]\Delta\widetilde{p}_o\\ &-\lambda_w\left(\Delta q^{p_o}_{\pm}\right) + \lambda_w\left(\Delta q^{p_c}_{\pm}\frac{dP_c}{dS_w}\Delta S_w\right) + \lambda_{g,w}\rho_{w,0}g(\Delta q^z_{\pm}),\end{aligned} \tag{19}$$

$$\begin{aligned}\Delta(\mathbf{u}^h_{o,f}\cdot\mathbf{n}_f) = &\left[\left(\frac{d\lambda_o}{d\widetilde{S}_w}\right)(-\mathcal{D}_1+\mathcal{D}_2) + \frac{d\lambda_{g,o}}{d\widetilde{S}_w}\mathcal{D}_{3,\alpha}\right]\Delta\widetilde{S}_w\\ +\left[\left(\frac{d\lambda_o}{d\widetilde{p}_o}\right)(-\mathcal{D}_1+\mathcal{D}_2) + \frac{d\lambda_{g,o}}{d\widetilde{p}_o}\mathcal{D}_{3,\alpha}\right]&\Delta\widetilde{p}_o - \lambda_o\left(\Delta q^{p_o}_{\pm}\right) + \lambda_{g,o}\rho_{o,0}g(\Delta q^z_{\pm}),\end{aligned} \tag{20}$$

where variation for the flux $q^y_{\pm}$ of the variable y is defined in Section 6.

8. NUMERICAL EXPERIMENTS

We consider two pseudo-2D numerical experiments, each uses three different flux discretization schemes: nonlinear multi-point, nonlinear two-point and linear two-point. Both test cases use the uniform $32 \times 32 \times 1$ grid for the compunational domain $[-50; 50] \times [-50; 50] \times [4000; 4010]$. The first experiment is for one injecting and one producing wells, and the second one is for three injecting and one producing wells.

Well locations are presented in Fig. 2. Injecting well pressure is equal to 4100 and producing well pressure is 3900.

Both experiments have been conducted for incompressible phases with constant viscosities $\mu_w = 1$, $\mu_o = 50$, constant porosity $\phi = 0.2$, zero capillary pressure and zero gravity terms, as required by the derivation of the discrete maximum principle Theorem 1. Relative permeabilities are shown in Fig. 3 and the absolute permeability tensor is:

$$k = R_z(-\theta_z)diag(k_1, k_2, k_3)R_z(\theta_z),$$

where $k_1 = k_3 = 100, k_2 = 0.1, \theta_z = 112.5°$, and $R_z(\alpha)$ is the matrix of the rotation in xy-plane.

Pressure for the two wells problem (Fig. 2, left) is presented in Fig. 4. The nonlinear multi-point scheme and the linear two-point scheme satisfy the discrete maximum principle for pressure as expected, while the nonlinear two-point flux discretization violates the discrete maximum principle. It was demonstrated in [3] that the mesh refinement reduces the magnitude of the overshoots and undershoots for the nonlinear two-point scheme, yet the DMP is still violated. In contrast to two nonlinear schemes,

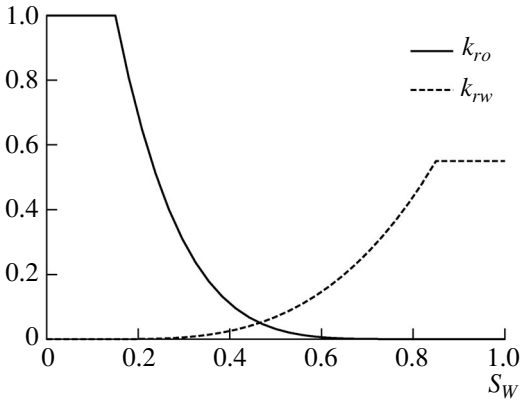

Fig. 3. Relative permeabilities.

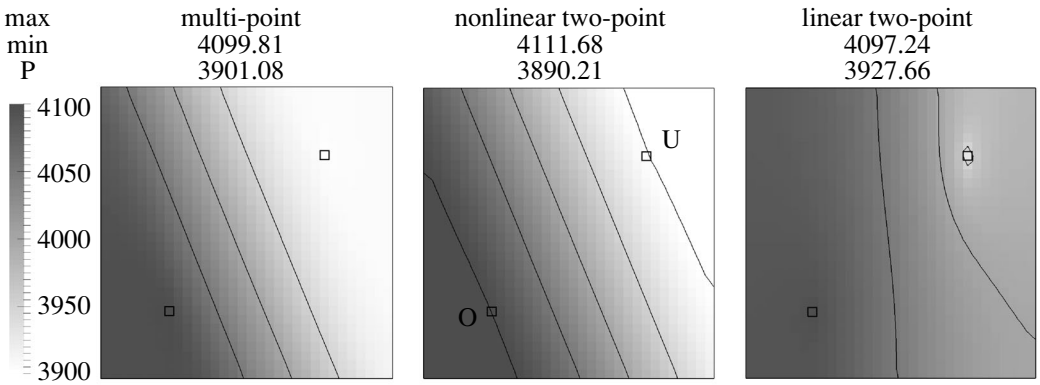

Fig. 4. Pressure for $t = 2000$ for different flux discretization schemes (numerical experiment with 2 wells). Overshoot ($p > 4100$) and undershoot ($p < 3900$) domains are denoted by O and U, respectively.

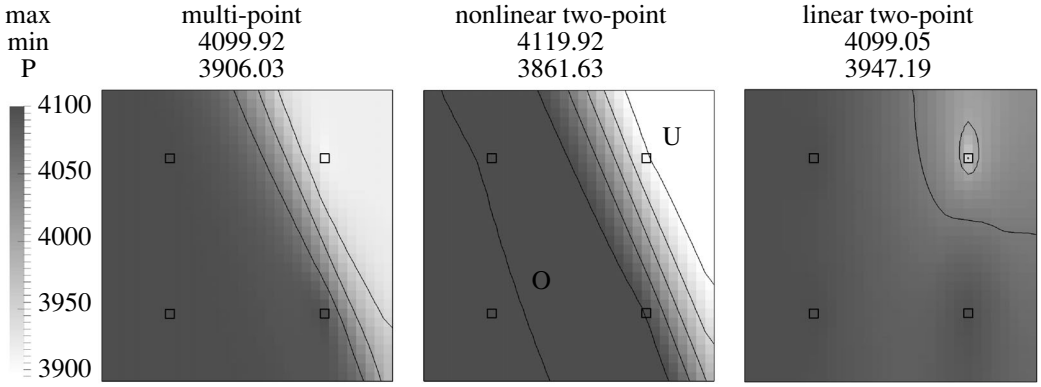

Fig. 5. Pressure for $t = 100$ for different flux discretization schemes (numerical experiment with 4 wells).Overshoot ($p > 4100$) and undershoot ($p < 3900$) domains are denoted by O and U, respectively.

the linear two-point scheme does not provide approximation for the fluxes which results in nonphysical pressure field: the solution is not aligned with the main anisotropy direction. Therefore, only the nonlinear multi-point scheme is consistent and satisfies the discrete maximum principle.

The four wells test case (Fig. 2, right) demonstrates the similar pressure solution violating the discrete maximum principle and the consequences of pressure DMP violation for the saturation solution. Fig. 5 shows the pressure solution for the time $t = 100$. Again, the discrete maximum principle is

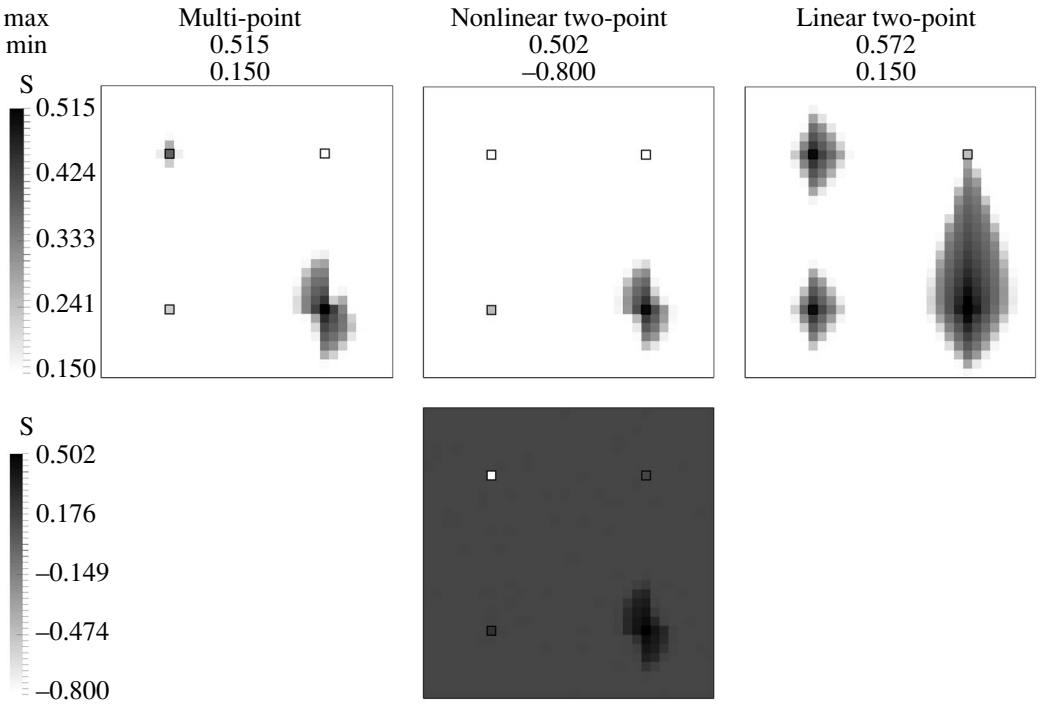

Fig. 6. Water saturation for $t = 100$ for different flux discretization schemes (numerical experiment with 4 wells). Bottom panel is colored according to extended saturation legend. Initial saturation is $s(0) = 0.15$.

violated by the two-point nonlinear scheme in the vast region. The top left injecting well cell has the overshoot and the pressure is higher than the well bottom hole pressure 4100. As a result the top left injecting well starts to pump out water instead of injecting. The nonphysical flow is magnified by the use of the downstream discretization of well mobility $\lambda_{inj} = (\lambda_w + \lambda_o)_{cell} > 0$, and water saturation of the well cell decreases even after it becomes zero. This leads to the nonphysical negative saturation on the top left well cell (see Fig. 6, middle), water saturation on this cell drops up to -0.800. Water saturations obtained by the multi-point nonlinear scheme, the nonlinear two-point scheme and the two-point linear schemes are compared in Fig. 6. Following the lack of the flux approximation of the linear two-point scheme the water flow is not alighed with the main anisotropy direction.

9. CONCLUSION

It was proved that under certain assumptions the nonlinear multi-point flux discretization scheme satisfies the discrete maximum principle for two-phase flow model. The scheme was implemented and the numerical results demonstrate that the solution for the pressure satisfies the discrete maximum principle in the cases where the monotone nonlinear two-point scheme fails. Unlike the conventional two-point linear scheme the nonlinear multi-point scheme preserves the flux approximation for the non-orthogonal grids and anisotropic permeability tensors. It was shown that the new scheme may be used with the Newton solver in fully implicit time discretization.

ACKNOWLEDGMENTS

The work was supported in part by RFBR grants 14-01-00830, 15-35-20991 and ExxonMobil Upstream Research Company.

REFERENCES

1. K. Lipnikov, D. Svyatskiy, and Yu. Vassilevski, "Minimal stencil finite volume scheme with the discrete maximum principle," Russian J. Numer. Anal. Math. Modelling **27**, 369–385 (2012).

2. A. Chernyshenko and Yu. Vassilevski, "A finite volume scheme with the discrete maximum mrinciple for diffusion equations on polyhedral meshes," in *Finite Volumes for Complex Applications VII: Methods and Theoretical Aspects* (Springer International Publishing, 2014), pp. 197–205.
3. A. Danilov and Yu. Vassilevski, "A monotone nonlinear finite volume method for diffusion equations on conformal polyhedral meshes," Russian J. Numer. Anal. Math. Modelling **24**, 207–227 (2009).
4. K. Nikitin, K. Terekhov, and Yu. Vassilevski, "A monotone nonlinear finite volume method for diffusion equations and multiphase flows," Computational Geosciences **18** (3) 311–324 (2014). doi 10.1007/s10596-013-9387-6.
5. Z. Sheng and G. Yuan, "The finite volume scheme preserving extremum principle for diffusion equations on polygonal meshes," J. Comp. Phys. **230** (7), 2588–2604 (2011).
6. L. Fraenkel, *Introduction to Maximum Principles and Symmetry in Elliptic Problems* (Cambridge University Press, 2000).
7. K. Aziz and A. Settari, *Petroleum Reservoir Simulation* (Applied Sci. Publ. Ltd, London, 1979).
8. D. Peaceman, *Fundamentals of Numerical Reservoir Simulation* (Elsevier, New York, 1977).
9. D. Peaceman, "Interpretation of well-block pressures in numerical reservoir simulation," SPEJ **18** (3), 183–194 (1978).